communications earth & environment

Article

A Nature Portfolio journal

https://doi.org/10.1038/s43247-025-03032-3

Coastal groundwater salinization impairs tree carbon–water balance

Yaling Zhang[1], Minhuang Wang[2] ✉, Josep Peñuelas[3,4], Jianming Xue[5], Zhiqun Huang[6], Xiaohua Gou[7] & Nate G. McDowell[8,9]

How coastal forest productivity varies with local nutrient availability and water supply remains a knowledge gap under climate change. In a two-decade field experiment manipulating fertilization and density in coastal pine forests, we show that a decade of growth enhancement by simulated sedimentary nutrient inputs has resulted in a striking reversal in growth and increased mortality risk as drought and sea level rise progressed. Recent groundwater salinization has further triggered a shift from nutrient to water limitation, causing severe stomatal closure and decoupling of tree carbon–water balance, which induces a negative intrinsic water use efficiency (iWUE)–growth relationship. Higher tree iWUE predicted sharper tree growth declines, and both nutrient enrichment and high stand density amplified this feedback, increasing the risk of hydraulic failure and mortality. These results suggest that a transient nutrient-stimulatory effect could drive further coastal forest degradation due to heightened belowground saltwater stress under sea-level rise.

Coastal regions harbor the Earth's most biogeochemically active ecosystems and nourish large populations worldwide[1–3]. Recent widespread vegetation retreats (e.g., growth decline and ghost forest formation) in these areas have emerged as a pressing concern facing coastal populations[4,5], which underscores the acute vulnerability of coastal ecosystems to climate change[6,7] and the uncertainty of associated carbon sink capacity[8–10].

Crucially, recent studies have reported widespread shifts from ecosystem energy to water limitation[11,12] and underlined the benefit of enhanced water-use efficiency for terrestrial vegetation growth[11,13,14]. As photosynthesis involves a trade-off between carbon uptake and water loss, tree carbon–water balance is essential for trees' growth and survival. A decrease in tree carbon–water balance may increase forest vulnerability to atmospheric or soil dryness and accelerate the risk of tree mortality once hydraulic failure couples with progressive carbon starvation[7,15]. As an indicator of this trade-off, tree intrinsic water-use efficiency (iWUE) often increased under rising atmosphere CO_2 (C_a) (13, 14) or drought events (15). However, increased iWUE has led to contrasting growth patterns[16–20], partly due to local water resource variability and its central role in mitigating forest response to climate change[19,21–23]. Uncertain interactions between climate and local resource availability limit our ability to predict coastal vegetation dynamics and functions[3,8,24–26].

Compared to upland terrestrial forests, water availability in low-lying coastal forests is more influenced by shallow groundwater depth, oceanic dynamics (e.g., oceanic evaporation and seawater–groundwater exchange), and salinity, which are some of the key constraints to coastal forest functioning[7,10,27]. The overexploitation of aquifers and recently accelerated sea level rise[4,28,29] have exposed trees to groundwater table declines or severe inundation and saltwater intrusion[6,7,30–32] in many coastal zones. As a result, anomalies in groundwater depth and chemistry can either subsidize tree water use or, in turn, induce salt stresses[1,5,6,15,33], leading to nonlinear influences on coastal nutrient biogeochemistry and ecosystem services[7,25,34]. For instance, groundwater anomalies or salinization may induce osmotic imbalances (e.g., lowering the soil-to-root water potential) that limit plant transpiration and cause hydraulic failure[15] from belowground[10], especially when atmospheric dryness shifts plant water use toward deeper sources[35]. Climate–groundwater interactions, closely intertwined with local water availability[33], may exacerbate the impacts of atmospheric drought (e.g., VPD)[24] on forest ecosystems; however, they have been historically

[1]Guangdong Provincial Key Laboratory of Applied Botany, South China Botanical Garden, Chinese Academy of Sciences, Guangzhou, China. [2]National-Regional Joint Engineering Research Center for Soil Pollution Control and Remediation in South China, Guangdong Key Laboratory of Integrated Agro-environmental Pollution Control and Management, Institute of Eco-environmental and Soil Sciences, Guangdong Academy of Sciences, Guangzhou, China. [3]CREAF Cerdanyola del Vallès, Barcelona, CT, Spain. [4]CSIC, Global Ecology Unit CREAF, CSIC–UAB Bellaterra, Barcelona, CT, Spain. [5]New Zealand Institute for Bioeconomy Science, Lincoln, New Zealand. [6]School of Geographical Sciences, Fujian Normal University, Fuzhou, China. [7]MOE Key Laboratory of Western China's Environmental Systems, College of Earth and Environmental Sciences, Lanzhou University, Lanzhou, China. [8]Atmospheric Sciences and Global Change Division, Pacific Northwest National Lab, Richland, WA, USA. [9]School of Biological Sciences, Washington State University, Pullman, WA, USA. ✉e-mail: mhwang@soil.gd.cn

neglected[26,34]. In light of regional hydrological heterogeneity and the growing risk of drought caused by atmospheric or soil dryness[1,6,27,32,36], unraveling how climate and local water regimes interact remains imperative to drive tree water use and growth dynamics in coastal areas[7,27].

Apart from water resources, environmental harshness reflected by other local stressors, such as nutrient availability, also interacts with climatic factors to alter the carbon–water cycles of plants[37–40]. Distinct from upland forests, nevertheless, coastal regions have received markedly increased rates of sediment inputs in many parts of the world, supplying abundant organic matter and nutrients for coastal vegetations, especially when sea level rise dominates[41]. Although high soil fertility promotes tree growth through adequate nutrient supply, it can decrease the hydraulic safety margin of trees by altering multiple hydraulic traits[37] or causing structural overshoot[42] that promote hydraulic failure and forest vulnerability to episodic water deficit. For instance, high nutrient inputs may, conversely, exacerbate salt-stress-induced hydraulic failure (impairing transpiration, root water uptake, etc.) and inhibit plant growth[43]. By contrast, resource shortages may constrain standing biomass increments and lead to self-thinning[44], i.e., density-dependent mortality driven by local tree competition. Local tree–tree interactions along the gradient of environmental harshness (nutrient and/or water stress) can induce either competitive exclusion (negative) or complementary facilitation (positive) to cope with resource shortages and other environmental stressors[45,46]. However, the importance of tree competition for tree growth can fall with increasing climatic/abiotic stress[47], thereby confounding the iWUE response to climate change and its consequences for tree growth[48–50]. Besides, depending on geomorphology and land use change by human activities, local coastal sediment inputs may also contribute contaminants such as heavy metals[41] that potentially impairing tree growth. To resolve these uncertainties (e.g., emerging from variations in water, nutrient, and resource competition), tackling the intricate interactions among climatic and local factors in coastal areas becomes crucial when upscaling the global carbon budget and projections[9,50].

To this end, we investigated tree annual growth rate in terms of basal area increment (BAI) and physiological changes (reflected by tree ring $\delta^{13}C$ and $\delta^{18}O$ data) of radiata pines (*Pinus radiata*) in a 20-year experiment established on a barrier island in Nelson City, New Zealand (Supplementary Fig. 1). This island, as a groundwater-dependent ecosystem, has poorly developed sandy soil and has been increasingly exposed to seawater intrusion in recent years[29], causing a potential nutrient and water use dilemma for tree growth. This experiment had a factorial design of repeated nutrient inputs (Nutrient treatment, from treated biosolids that simulated continuous inputs of eutrophic estuarine sediments in coastal areas) × manipulated stand density levels (Density treatment), coupled with long-term monitoring of groundwater level and chemistry, providing a great opportunity to experimentally test how climate and local stressors interact to modulate carbon–water balances during tree growth and mortality (see a conceptual diagram in Supplementary Fig. 2). For this study, we used the field data to test whether coastal forests can initially benefit from nutrient enrichment through the inputs of eutrophic estuarine sediments in coastal areas and increased atmospheric CO_2 as illustrated above; nevertheless, because enhanced tree growth is often accompanied with higher water demand, the impact of groundwater salinization on tree growth under sea level rise could be more pronounced in later years compared to the earlier years. Therefore, by focusing on tree carbon–water balance, we hypothesize that (H1) mismatches between growth enhancement and local water scarcity resulting from groundwater salinization would cause a shift from nutrient to water limitation, leading to negative iWUE-BAI feedback, particularly for trees in fertile sites or crowded stands. We further hypothesize that (H2) such negative iWUE-BAI feedback is linked to a strong decoupling between tree carbon and water balance in the later period, leading to increased tree mortality rate.

Materials and methods

Study site

The experimental site was established in 1997 in a *P. radiata* forest plantation (planted in 1991) on a flat coastal barrier island (altitude <10 m) (Supplementary Fig. 1) situated near Nelson City, Tasman Bay, New Zealand. The soil in the area is classified as sandy raw soil with low levels of organic material and soil fertility. This soil is permeable and provides free rooting access to shallow groundwater 2.0–4.2 m below the surface. The coastal zones near Tasman Bay are vulnerable to seawater intrusion due to rising sea levels (rose by 2.84 ± 0.18 mm per year between 1961 and 2020, recorded at the closest monitoring site), substantially increasing groundwater salinity[28]. The field trial consisted of a split-plot, randomized block design with four replicated main plots applied with three levels of treated biosolids (i.e., stabilized domestic sewage sludge containing ~3% total solids) every 3 years (1997, 2000, 2003, 2006, 2009, and 2012): (1) control (no biosolids), (2) N300 treatment (300 kg N ha^{-1}), and (3) N600 treatment (600 kg N ha^{-1}) (Supplementary Fig. 1). Each main plot consisted of three tree stocking rates (subplots) at 300, 450, and 600 stems ha^{-1}. There were 36 subplots, each measuring 25 × 25 m, plus 5-m buffer zones. We used the basal area of each plot (plot BA) to represent tree competition intensity when employing competition as a continuous variable, as was done in previous studies[48]; however, for better graphic visualization, we also used the stand density treatment (i.e., D300, D450, and D600) as a categorical variable.

We intensively monitored multiple plant and soil responses to assess the ecological impact of repeated organic and nutrient inputs from treated biosolids. Plots were censused every year between 1997 and 2015, and tree growth and mortality were regularly monitored. We measured the diameter at breast height of live trees in each subplot and calculated the total live tree BA (plot BA) and BAI for each subplot. We estimated the annual stem density and annual stem mortality by counting the number of stems per hectare in each census and the number of stems lost in each census interval, respectively. We conducted a final survey in 2021 on harvesting trees at the experimental site. We assessed leaf N concentration by sampling the current-year needles of radiata pines in 1998–2015 (but not in 2012 and 2014) for each main plot (i.e., fertilization treatment). Leaf N is used as a common surrogate for photosynthetic capacity; in this study, it was used to reflect photosynthetic capacity because of the enzymatic N demand required to have a high photosynthetic capacity[51].

Tree ring chronologies and stable isotope ratio analysis (δ13C and δ18O)

In May 2015, we sampled wood cores and developed tree ring chronologies (spanning 1995–2015) in the *P. radiata* stands by taking pith-to-bark cores at breast height using an increment borer (bore diameter: 5 mm) from four target trees in each of the 36 subplots (in total 144 cores, i.e., 48 cores per fertilization treatment or per density level). To better capture the current-year tree physiological response to climate and environmental changes, we used only latewood for stable isotope analyses to eliminate the signal influence from the previous year.

Tree-ring samples were ground and extracted for α-cellulose, and the samples of which were then analyzed for $\delta^{13}C$. We applied a correction method[52] to the raw data to obtain the corrected values ($\delta^{13}C_{corr}$) by removing the influence of increasing C_a. We further pooled α-cellulose samples to reduce replicates (by combining four main-plot replicates for each biosolids × density treatment) used for $\delta^{18}O$ analysis.

Carbon isotopic discrimination and tree iWUE calculation

The carbon isotopic discriminations (Δ) of the tree ring $\delta^{13}C_{corr}$ data were calculated as $\Delta^{13}C = (\delta^{13}C_a - \delta^{13}C_p)/(1 + \delta^{13}C_p /1000)$, where $\delta^{13}C_a$ and $\delta^{13}C_p$ are the $\delta^{13}C$ values of air and plant tissue, respectively. We obtained the $\delta^{13}C_a$ value from the most recent records of the annual mean $\delta^{13}C_a$ measured in Mauna Loa, Hawaii. Following Farquhar et al.[53], we calculated intrinsic water-use efficiency (iWUE) using two equations. The ratio of the CO_2 inside the leaf (c_i) to CO_2 in the atmosphere (c_a) was derived from $\Delta^{13}C$ as

$$\Delta^{13}C = a + (b - a) \times (C_i/C_a),$$

where a is the fractionation of $^{13}CO_2$ during diffusion in air through stomata (4.4‰) and b is the net biochemical fractionation during photosynthesis (27‰); Solving for c_i and the c_i/c_a ratio, we then calculated the intrinsic water use efficiency (iWUE) of the focal trees[54]:

$$iWUE = A/g_s = (C_a - C_i)/1.6,$$

where 1.6 is the ratio of diffusivities of c_a to water vapor. A and g_s denote foliar stomatal conductance and C assimilation rates, respectively.

Climate, oceanic, and local environmental parameters

We obtained regional mean annual climate and sea level data, including temperature, precipitation, and sea level rise, for the Nelson region (New Zealand) from the website of the National Institute of Water and Atmospheric Research (NIWA), New Zealand (https://niwa.co.nz). We obtained mean annual data for oceanic evaporation and the multivariate ENSO index (MEI) from the NOAA Climate Data Record. For the entire study period, we quarterly conducted site-specific local observations of groundwater table depth and groundwater quality via eight monitoring wells installed at our experimental site (Supplementary Fig. 1).

Statistical analysis

Based on general additive models (GAMs), we first fit and visualized trends in tree growth rates, physiological traits, and basic environmental predictors. The use of GAMs, with smooth spline predictor functions incorporated into the generalized linear model (GLM) framework, helps examine the long-term patterns in both responsible and explanatory variables. We then used a changepoint analysis (segmented R package) to test whether the changes in BAI had nonlinearly shifted over the past two decades and, if so, to identify the transitional year in which the tipping point was reached. Using data from all plots, we identified a tipping point from a positive to a negative temporal trend in BAI shifts in 2005, which thus separated the time series into two phases: the earlier (1995–2005) and later (2005–2015) periods. The potential drivers of annual tree growth in each of the two stages were then further analyzed. Likewise, we applied the same stage separation when exploring the factors driving the changes in the iWUE.

To explore the potential drivers of tree growth and iWUE in these two distinct stages, we used boosted regression trees (BRTs) implemented in the gbm R package to overcome the complex effects of multiple predictors on response variables. We used "C_a", "iWUE", "fertilization level", "plot BA", "groundwater salinity", "groundwater level", "oceanic evaporation", "application replicates", "sea level rise", "mean annual MEI", "SPEI", "mean annual temperature" and "mean annual precipitation" as explanatory variables for BAI and iWUE (but not "iWUE" in the latter case). The BRTs provided us with the major climatic and local predictors and their relative importance to tree growth and iWUE. Partial dependence functions were also calculated to better visualize the relationship between the predictors and the response variables. Finally, we used the structural equation model (SEM) to investigate the direct and indirect (mediated by tree physiological effects, here refer to iWUE and $\delta^{18}O$) pathways by which climate and local factors interacted to drive coastal tree growth separately for early and later periods (a conceptual diagram in Supplementary Fig. 2). Following Craine et al.[55], we also conducted an overall SEM using all observations that used residual BAI after accounting for accounting for Year Effect and its break point at 2005. SEM models were implemented in the R programming language using the lavaan package (version 0.6.16, no customized modification indices were used).

Results

Global and local environmental predictors

During the experimental period (1995–2015), global ambient atmospheric CO_2 constantly increased from 360 mol mol^{-1} to 400 μmol mol^{-1} (~11% increase, data from Mauna Loa Observatory, Hawaii) (Fig. 1a). Oceanic evaporation varied in early years, with a sharp decline since 2005 (Fig. 1b). Mean annual temperatures (MAT) tended to increase despite considerable high interannual variations (especially before 2005) (Fig. 1c). Regional sea level has increased at a slower rate since the late 1990s, with a sharp rise after 2008 (Fig. 1d). Corresponding to rising sea levels, groundwater salinity, as reflected by groundwater PC1 (the first component of PCA, representing salt chemistry, e.g., electrical conductivity, magnesium, calcium, sodium, etc.; see Supplementary Fig. 3), remained marginally constant until a dramatic increase was noted since 2008 (Fig. 1e). Groundwater PC2 (the second component of PCA, representing water level depth, nitrogen, pH; see Supplementary Fig. 3) tended to decrease before 2008, except for a high level of range variations in 2008; then it mainly increased in the later 3 years (Fig. 1f). In general, the salinity level and other properties of groundwater increased exponentially with rising sea levels (Supplementary Figs. 4, 5). The long-term standardized precipitation-evapotranspiration index (SPEI), multiple Enso index (MEI), and mean annual precipitation showed a dynamic temporal trend during this period (Supplementary Fig. 6).

Tree growth rates, iWUE, the iWUE–growth relationship, and their predictors and consequences for tree mortality

In terms of BAI, tree growth rates in our experimental sites displayed hump-shaped patterns, with a maximum growth-rate peak in 2008 for the control treatment and in 2005 for the standard and high treatments, respectively (Fig. 2a). Following these peaks, the BAI slope in the fertilized plots dropped more significantly, and stem growth rates across the different treatments converged to a comparable level after 2012 (Fig. 2a). While further analyzing separated experimental phases (earlier *versus* later periods separated by the year 2005), we found that atmospheric CO_2 concentration and fertilization levels ranked as the two most important drivers of BAI during the earlier period (1995–2005). By comparison, stand density became the primary driver of BAI in the later phase (2005–2015) (Supplementary Fig. 7).

With rising CO_2, contrary to common straight positive responses, we found that tree iWUE varied moderately at a rate of 0.265 ± 0.06 μmol CO_2 mol^{-1} H_2O per year before 2005; however, it sharply increased at a rate of 1.88 ± 0.18 μmol CO_2 mol^{-1} H_2O per year in later years (Fig. 2b). In particular, we statistically identified the breakpoints of tree iWUE in 2005, corresponding to the peaking point of the tree growth rate at the population level. Following the rise of iWUE after 2005, the Nutrient treatment caused a significantly higher iWUE increment than that in the control (Fig. 2b). However, we observed no significant impacts of density on tree iWUE. From 1995 to 2005, air temperature primarily determined tree iWUE, whereas after 2005, groundwater salinity outcompeted climatic factors and became the predominant factor positively driving tree iWUE (Supplementary Fig. 8).

The opposite trend of iWUE and tree BAI after the peaking point led to an overall negative relationship between iWUE and tree growth rate ($k = -0.387$), with weak responses in control and D300 but strengthened negative relationships in the high-N and high-density treatments (Fig. 2c). Coinciding with the negative iWUE-BAI feedback, tree mortality significantly increased after 2005 (Supplementary Fig. 9). Intriguingly, high Nutrient treatment and high density significantly increased plot-level tree mortality rates by up to twofold (control: 1.86%, N300: 2.42%, and N600: 5.61%) and fourfold (Density-300: 1.14%, Density-450: 2.76%, and Density-600: 6.00%), respectively (Fig. 2d and Supplementary Table 1).

Tree physiological responses

In the earlier period, the values of carbon isotope ratio ($\delta^{13}C$), C_i, C_i/C_a, and oxygen isotope ratio ($\delta^{18}O$) varied between different years, albeit with minor differences across Nutrient treatments or tree density levels (Fig. 3a–d; Supplementary Fig. 10a–d). C_i rose proportionally to C_a (0.576 ppm per ppm of C_a), resulting in relatively constant C_i/C_a ratios (slope marginally equal to 0, i.e., −0.0006 ~0.0001; Fig. 3b, c).

In the later period, the range of variations in tree physiological plasticity indicators decreased over the years, despite divergence across different Nutrient treatments (Fig. 3a–d). The values of $\delta^{13}C$ increased at a greater rate with rising C_a by 0.91 ± 0.08 μmol CO_2 mol^{-1} H_2O per ppm of C_a, whereas C_i decreased with greater C_a: for each increase of 1 ppm of C_a, the C_i

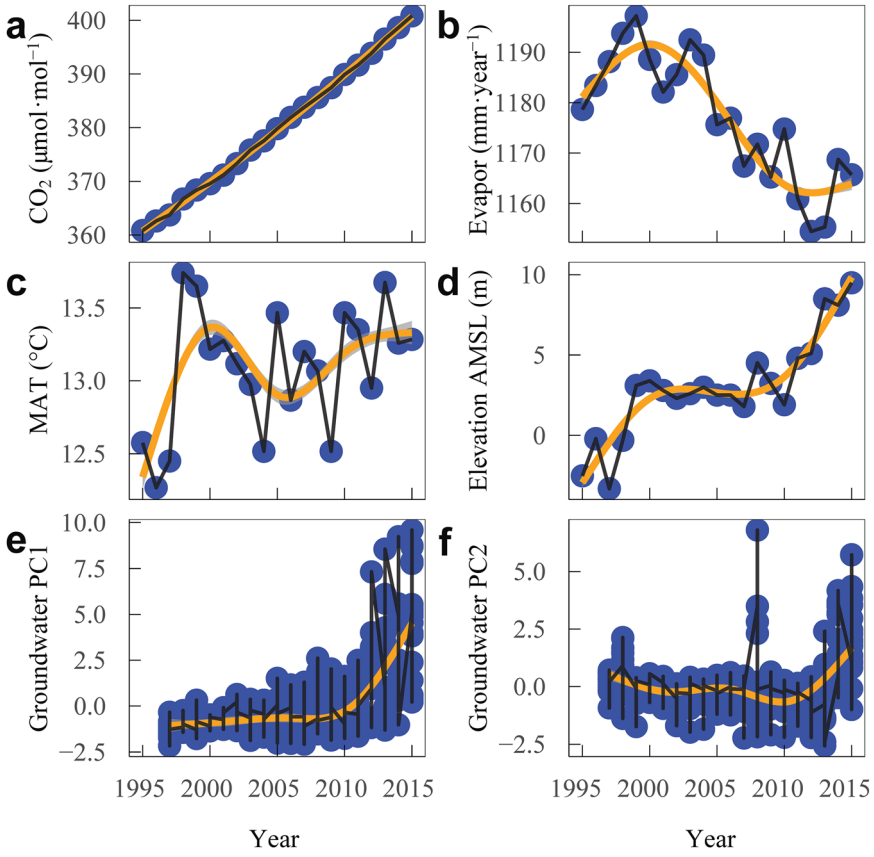

Fig. 1 | Two-decade trends in oceanic factors and local groundwater dynamics. Time series of (**a**) atmospheric CO_2 concentrations, **b** globally averaged oceanic evaporation, **c** mean annual temperature (MAT), **d** regional sea level (a.m.s.l.), **e** the PC1 scores of plot-level groundwater properties, and **f** the PC2 scores of plot-level groundwater properties are shown. Note that groundwater PC1 is primarily contributed by magnesium, calcium, conductivity, sodium, and chloride of groundwater, while groundwater PC2 summarizes the variations in water level depth, NH_4^+, pH, and NO_3^-.

decreased by 0.45 ppm (Fig. 3a, b). This declining trend of C_i and C_i/C_a ratios was significantly enhanced by the Nutrient treatment; however, it was not affected by tree density levels (Fig. 3b, c; Supplementary Fig. 10b, c) and represented strong stomatal regulation. This strong physiological response translated into a sharp increase in iWUE, with groundwater salinity as the predominant factor (Supplementary Fig. 7). $\delta^{13}C$ and $\delta^{18}O$ data also indicated that groundwater salinity played an important role in stomatal regulation. In particular, the values of the tree ring isotopes ($\delta^{13}C$ and $\delta^{18}O$) are positively correlated with rising sea levels and groundwater salinity (reflected by electric conductivity) (Supplementary Fig. 11). Notably, we found a significantly positive relationship between $\delta^{18}O$ and iWUE in the earlier period; however, this relationship was decoupled in the later period (Fig. 3f). The $\delta^{18}O$ values increased significantly with rising C_a by 0.090 ± 0.010‰ per ppm of C_a during the earlier period but remained relatively constant (slope equal to 0.010 ± 0.004, Fig. 3d) during the later period. We found no significant linear trends in leaf nitrogen (N) concentrations in Nutrient treatments but a concave-positive trend in the control over the calendar years (Fig. 3e; Supplementary Fig. 12).

Structural equation modeling (Fig. 4a) further confirmed positive direct effects of climate and nutrient availability (Nutrient treatment), but the associated indirect paths through regulating tree iWUE and stomatal optimality ($\delta^{18}O$) are not significant in the early period. At this stage, the negative impact of groundwater anomaly on tree growth is only marginally significant (Fig. 4a). By contrast, we found significant negative effects of groundwater and climate on tree growth rate through indirectly regulating iWUE, and the negative influence of groundwater on tree growth strengthened (Fig. 4b). Notably, we found that the covariation relationship between iWUE and $\delta^{18}O$ diminished in the later period, but the influences of local factors (Nutrient treatment, groundwater, and tree density) considerably enhanced in the later period compared to those in early period (Fig. 4). In together, the total effects of local factors are comparable to climate factors on coastal tree growth, with stronger indirect climate-stomatal feedback whereas stronger direct effects of local factors (Supplementary Fig. 12).

Discussion

Our results uncover an emergent scenario about how climate change indirectly impacts coastal vegetation dynamics, i.e., water/salt stress from sea level rise-driven groundwater salinization coupled with atmospheric dryness, with nonlinear detrimental impacts on plant transpiration and growth[34]. Tree growth was accelerated in the earlier period (before 2005) by high nutrient availability and rising atmospheric CO_2. In the later period (after 2005), tree growth declined due to the rise of sea level rise-driven groundwater salinization, exacerbating the increased atmospheric dryness feedback on stomatal efficiency in carbon gains. Thereafter, the episodic dryness strengthening by interactions between climate and local groundwater regimes compromised tree carbon–water balance, with quick consequences for coastal forest growth and mortality.

Specifically, as shown in SEMs (Fig. 4), nutrients exhibited a significant positive direct effect on tree growth during the initial phase, while climate and groundwater exerted direct positive and negative influences on tree growth, respectively, with the climatic effect being more pronounced. Although both factors impacted intrinsic water-use efficiency (iWUE), alterations in iWUE did not correspond to growth responses; during this period, iWUE remained closely associated with $\delta^{18}O$ (indicating relatively optimal carbon–water balance) and was not affected by nutrient levels, which also induced an indirect negative effect on tree growth through stand density, suggesting that nutrient limitation may more strongly constrain growth than water availability. In the subsequent phase, as atmospheric moisture availability and groundwater levels declined concurrently, the direct effect of climate on growth became negative, and the effects of groundwater intensified significantly. Climate and groundwater collectively suppressed tree growth by substantially modulating negative iWUE-growth relationships. The direct growth-promoting effect of nutrients also

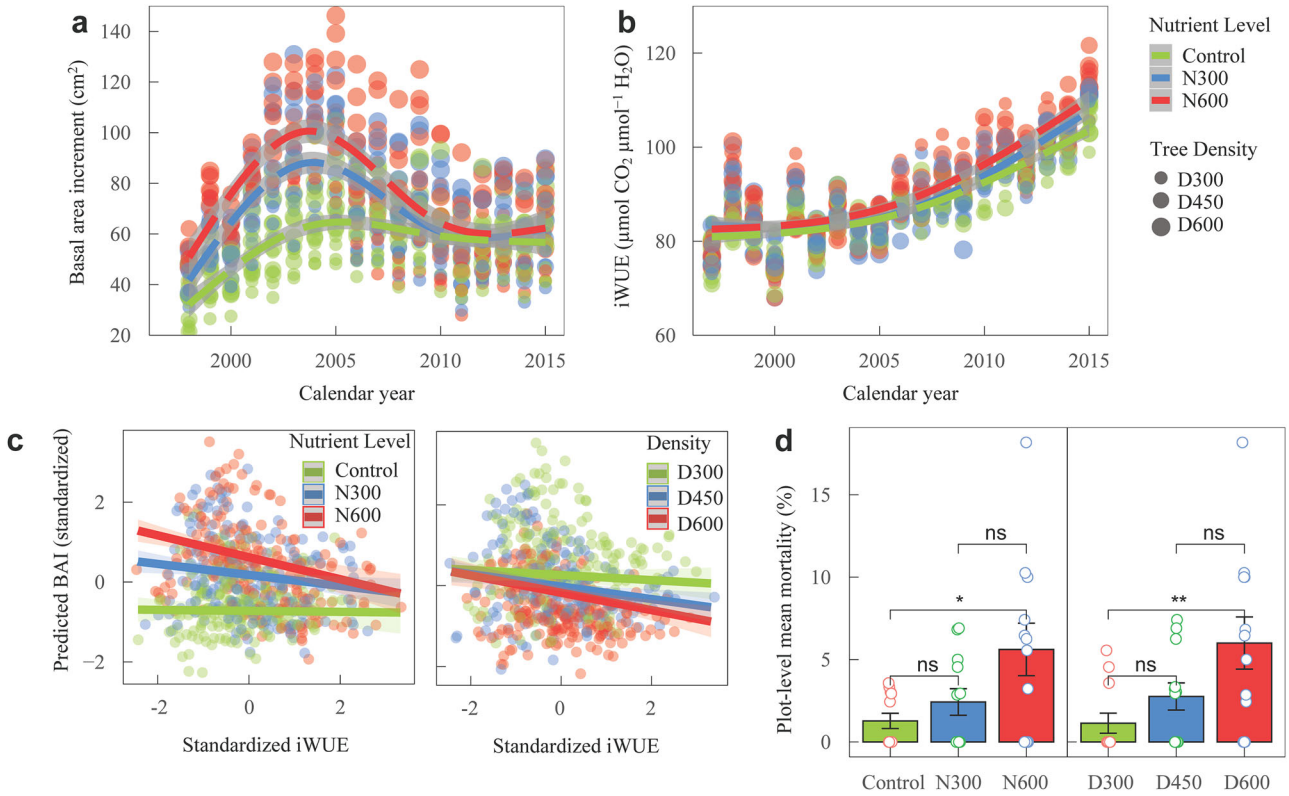

Fig. 2 | Tree growth, water use efficiency, and mortality rate across different levels of Nutrient treatment and tree density. In the (**a**) hump-shaped patterns of annual basal area increment (BAI) and (**b**) nonlinear trends of tree iWUE across different Nutrient × density treatments over two decades are shown. In (**c**), the relationship between BAI and iWUE (both of which are fitted with standardized data, i.e., Z-scores) is separately predicted for the Nutrient input treatment and stand density using linear mixed effect models with block as a random effect; and (**d**) plot-level mean mortality rates in different Nutrient treatments and in different density levels are shown. GAM regressions ($k = 4$) are fitted for the BAI and iWUE data, while the trend and the significance of treatment effects on tree mortality rates are predicted from hurdle GLMM models (see Supplementary Table 1).

disappeared, accompanied by a positive nutrient effect on iWUE. Nutrients often raise the maximum leaf photosynthetic capacity and mesophyll conductance, so for a given stomatal conductance, leaves assimilate more carbon, thereby increasing iWUE (A/gs) and making this effect proportionally larger under water limitation when gs is constrained[56,57]. This indicates that water limitation progressively surpassed nutrient limitation as the primary growth-limiting factor (Supporting **H1**).

The positive nutrient effect on iWUE may temporarily alleviate drought-induced growth and metabolic impairments or delay photosynthetic failure, as signals of short-term physiological acclimation to environmental stress[57], yet it is not by itself proof of long-term adaptation and often fails to prevent growth declines under progressive drought. This regime transition of resource limitations led to a marked reduction in growth as individuals that had previously thrived under conditions of high nutrient or stand density levels became increasingly susceptible to progressive water stress. The heightened water limitation also disrupted the relationship between iWUE and $\delta^{18}O$, thereby undermining the original carbon–water balance, which preserves hydraulic function and sufficient carbon for maintenance by stomatal closure, modestly reducing photosynthesis and water transpiration together[58]. However, prolonged drought can induce hydraulic failure processes (e.g., xylem embolism, root conductivity loss) or constraints on carbon transport and use (e.g., impaired phloem transport, prolonged negative carbohydrate balance) that decouple carbon and water supply[7,58]. These interacting pathways from hydraulic-failure to carbon-starvation impaired tree carbon–water balance and ultimately resulted in a significant increase in mortality (Supporting **H2**).

The observed growth decline and accelerated mortality generally corroborate the declining land carbon sinks globally[20] and specifically in New Zealand when confronted with a warmer and drier environment. The early growth peak in fertile sites in turn led to faster feedback in growth decline, with relatively high mortality similar to crowded sites, which supported a local resource-driven asynchrony of regional carbon sink saturation[59]. Moreover, climate-boosted coastal tree growth may have encountered a specific resource or ontogenetic threshold[60] other than soil fertility[61]. Particularly, mismatches between (fresh) water demand and saline groundwater supply in these areas have decoupled positive feedback between tree carbon and water balance and thus increase the risk of hydraulic failure and mortality. These findings advance current observational-level knowledge on how local water regimes may counteract climate change to determine coastal forest dynamics[9,34] and their carbon sink capacity[8].

Local resource- and stage-dependent growth responses to climate change

Coastal pine forests in these areas faced no severe air drought (no significant decline trend in oceanic evaporation) before 2005 (Fig. 1b), and sea level rise-driven groundwater levels and salinity also varied at minimal rates, indicating marginal water/salt stress from groundwater salinization (Fig. 1d–f; Supplementary Fig. 5). Therefore, water availability is not likely a primary limiting factor for growth (Supplementary Fig. 7); in support of this, the intrinsic water-use efficiency (iWUE) of the pine forests only slightly increased, with air temperature being the main driver in this period (Fig. 2b; Supplementary Fig. 7). Instead, we documented strong stimulation of tree growth by high nutrient availability in the earlier period under elevated atmospheric CO_2 and temperature (Fig. 2a). The is consistent with previous studies noting that temperature variability[62] and nutrient availability exert strong control over trees' photosynthetic responses to elevated CO_2[63,64],

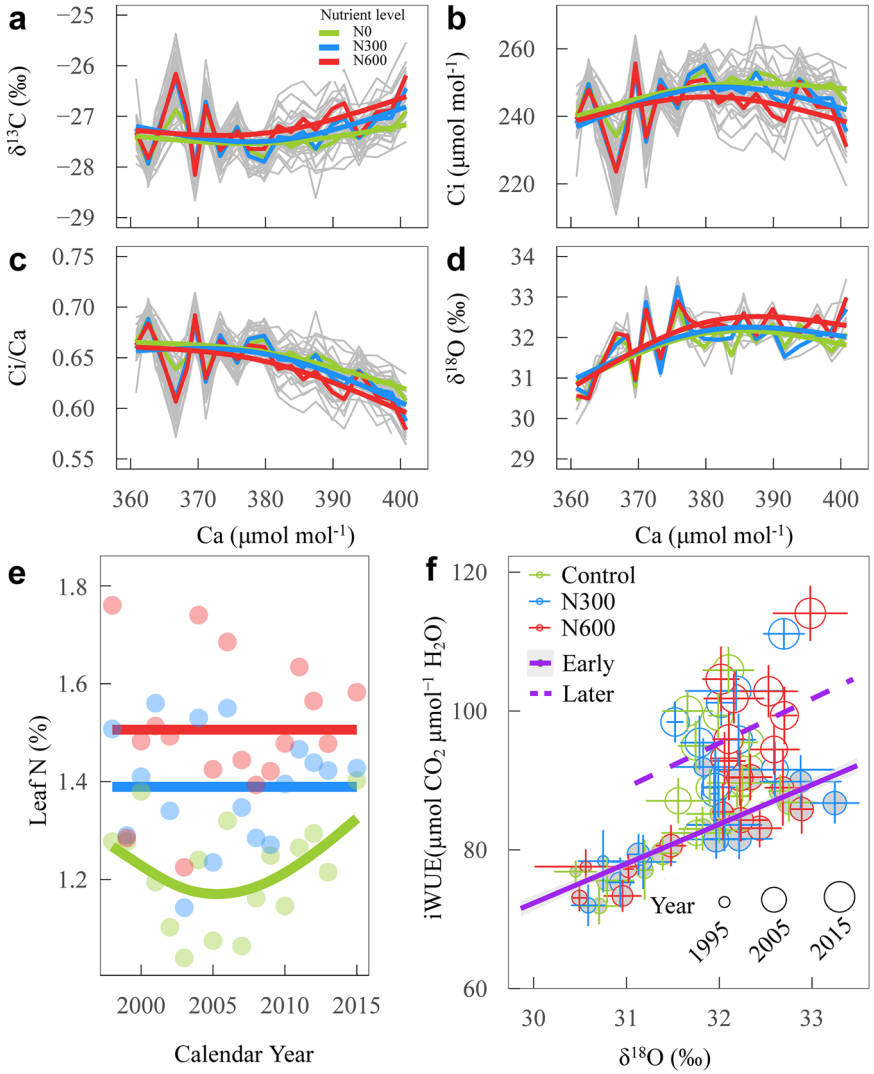

Fig. 3 | Tree physiology, leaf N content and the $\delta^{18}O$-iWUE coupling relationship. Temporal variation in the annual values of (**a**) carbon isotope ratios ($\delta^{13}C$), **b** intracellular CO_2 concentrations, **c** the ratio of intracellular [CO_2] (Ci) to atmospheric [CO_2] (C_a), and **d** oxygen isotope ratios ($\delta^{18}O$) in response to rising atmospheric CO_2 concentrations (C_a) during the tree ring chronological period (1995–2015). Lines of different colors represent annual mean values for different biosolid treatments, and smooth lines are fitted by GAM regressions (C_a equals around 380 μmol mol^{-1} in the year 2005); **e** Temporal changes in leaf N content across the nutrient input treatments; **f** Relationships between tree ring oxygen isotopic ratio ($\delta^{18}O$) and iWUE of radiata pine trees at our study site in early (gray-solid points) and later periods (blank points). Early period: the solid purple line represents one significant slope of a theoretical, positive relationship between $\delta^{18}O$ and iWUE if stomatal conductance was a greater determinant of Ci (CO_2 concentration in the intercellular spaces of leaves) than photosynthetic capacity; Later Period: the dashed purple line represents a nonsignificant association. Bars are 1.0 SE.

suggesting that nutrient limitations in these infertile coastal sandy soils could prevent the full expression of the increasing CO_2 effect on tree growth[61,65,66].

After 2005, a sharp decline of oceanic evaporation indicated accelerated atmospheric dryness in these areas (Fig. 1b) and may compel coastal trees to rely on deeper soil water[35]. The steeper increase in groundwater levels and salinity after 2008 implies a turning point of intensified seawater intrusion (Fig. 1d–f; Supplementary Fig. 5), posing a water-use dilemma for coastal trees. Prolonged salinity stress, akin to aridity[67], limits plant transpiration and causes physiological dysfunction, being more instantaneous than other climatic drivers (Supplementary Fig. 7d) due to osmotic stress and direct inhibition of root water uptake[7]. A previous study has shown that seawater intrusion can constrain tree growth and gas exchange in coastal forests[30]. Groundwater over-extraction and climate change effects, particularly the continuing drought and rises in sea levels (Fig. 1c, d), have increased both the risk and the intensity of seawater intrusion in many of New Zealand's coastal aquifers[28,29]. The coastal margin of the Waimea Plains that lie inland from our experimental site on a barrier island has become vulnerable to seawater intrusion in recent years[29]; hence, it is likely to cause a long-lasting decline in tree radial growth (Fig. 2a). According to a conceptual model based on tree-ring proxies[68], continuous growth declines can entail tree mortality due to carbon starvation and carbon-mediated hydraulic failure, as supported by the significantly enhanced mortality in the later period (Supplementary Fig. 9). However, research often overlooks local-specific disturbances[23], such as seawater exposure in low-lying areas[15,21], and the potential impact of groundwater/soil porewater salinity[15] on coastal vegetation declines. Therefore, we stress the episodic interplay of climatic and local factors in predicting coastal vegetation dynamics, emphasizing the developmental local factors, such as groundwater anomaly, as a neglected dimension.

Nonlinear physiological responses to interactions between climate and local factors

We further demonstrate physiological evidence pointing to a nonlinear detrimental effect of groundwater salinity on the integrity of tree carbon–water relations, evolving along with accelerated sea level rise and rising atmospheric aridity[12,36]. Guided by the least-cost ecological optimality hypothesis, trees strategically balance investments in transpiration capacity and maximum carbon assimilation rate to optimize photosynthesis at the lowest total cost, encompassing growth and maintenance respiration[69,70]. Physiological signals gleaned from tree-ring chronologies provide insights into carbon–water balances in low-lying coastal forests amid intricate soil–plant–atmosphere interactions[3,4]. Trees strategically regulate their stomatal aperture to ensure optimal intercellular CO_2 concentrations (C_i) in photosynthesizing tissues, causing carbon and oxygen isotope discrimination (reflected by $\delta^{13}C$ and $\delta^{18}O$ data) when optimizing C_i[71]. In the earlier period, we observed highly variable patterns of $\delta^{13}C$, C_i, C_i/C_a ratios and $\delta^{18}O$ across years but not of Nutrient treatments (Fig. 3a–d), suggesting

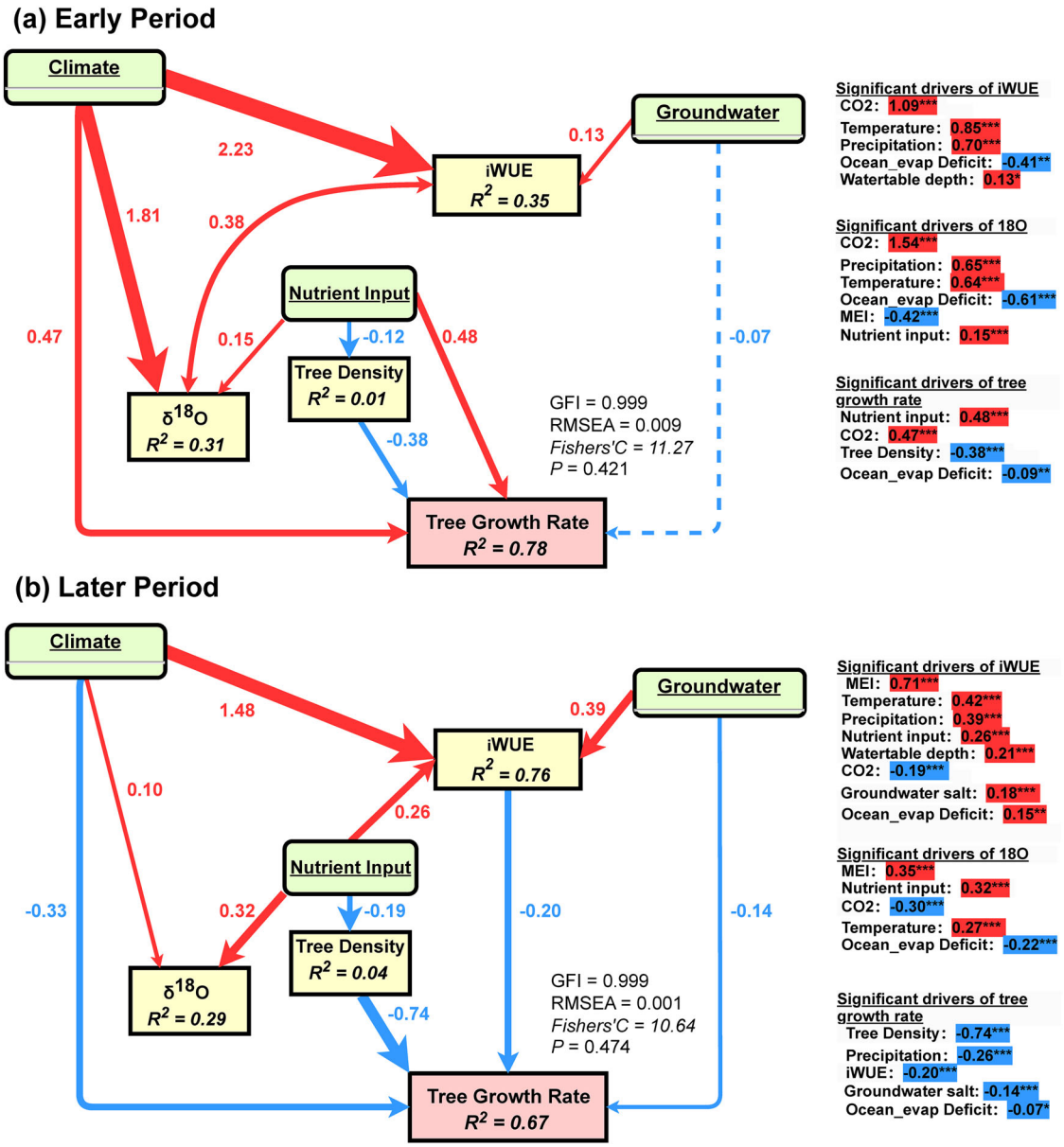

Fig. 4 | The relationship between climate, local factors (nutrient level, stand density, groundwater properties), tree physiology (iWUE/ $\delta^{18}O$), and tree growth rate. The final SEMs disentangling the direct and indirect iWUE/ $\delta^{18}O$-mediated effects of climate or local controls on tree growth rates for (**a**) the early period and (**b**) the later period. For simplicity, we grouped the effects of climate drivers and groundwater properties on tree growth, respectively, but it does not represent latent variables (see Supplementary Tables 2, 3 for summary details of the full SEMs). The arrow thickness of different pathways represents the magnitude of the standardized regression coefficient (see estimates shown adjacent to arrows). R^2 for modulators and the final component is also given.

loose stomatal regulation to maximize carbon uptake and cope with climate fluctuations[16,72]. Evidence from tree-ring $\delta^{18}O$ at our experimental site supports this interpretation. According to dual-isotope theory, the ^{18}O composition of tree rings is unaffected by photosynthetic activity and reflects only variability in transpiration and stomatal conductance (g_s)[71]. Hence, the highly variable patterns in tree ring $\delta^{18}O$ indicate flexible stomatal regulation in the early period.

With coupled atmospheric and groundwater-related aridity in the later period, these coastal pines should optimize their priority between water savings and photosynthetic capacity[51,70,73], and we witnessed a shift toward severe stomatal closure (i.e., substantial reduction in g_s) and photosynthetic inhibition. Uncommon declines in C_i/C_a ratios and constant $\delta^{18}O$ values, with lower interannual variation (Fig. 3b–d), suggested tighter stomatal regulation and potential losses in stomatal sensitivity and photosynthetic flexibility to climate fluctuations. The decreased trend in C_i reported here implies even greater physiological responses than those in which C_i remains constant, which is strongly associated with increasing water stress[16,72,74]. Increased water limitation typically triggers stomatal closure and ultimately leads to increased $\delta^{13}C$ (Fig. 3a), indicating a relationship between plant stress responses and local water availability[74]. $\delta^{13}C$ increased significantly in the later period, a process observed in other coastal forests after seawater exposure[30,31].

Notably, severe reductions in g_s were expected to theoretically increase the $\delta^{18}O$[71], yet we observed slightly lower and constant $\delta^{18}O$ in the later period (Fig. 3d). Similar constant $\delta^{18}O$ values have also been reported in Japanese coastal freshwater ecosystems following tsunami-induced seawater intrusion[31] and post-drought pine forests (*Pinus. sylvestris* and *Pinus. nigra*) in Spain. Given the overall positive relations between tree ring $\delta^{18}O$ and tree growth rate (Fig. 4), on the one hand, the relatively constant lower overall $\delta^{18}O$ values in these pines suggest that such an exchange may have

reached carbon–water equilibrium[75]. On the other hand, constant $\delta^{18}O$ values indicated that they probably reached the minimum stomatal conductance to lower water loss and maintenance cost[73], corroborating the least-cost optimality hypothesis[69,70]. Herein, however, the later uncoupling between iWUE and $\delta^{18}O$ (Fig. 3f) indicated that the carbon sink process is mainly driven by photosynthetic capacity rather than by stomatal regulation[76], positing a potential loss of stomatal flexibility or reliance on deeper soil water sources. The slightly decreased $\delta^{18}O$ has been attributed to the increased contribution of ^{18}O-depleted xylem water with salinity compared to leaf water[75] to the post-photosynthetic exchange of carbonyl oxygens during cellulose synthesis[77]. The ^{18}O-depleted xylem water often requires substantial subsidies from deeper water resources, which are more depleted in terms of $\delta^{18}O$ than topsoil water due to lower exposure to evaporative isotopic enrichment[78].

Besides, we found evidence that the positive effect of nutrient inputs on tree growth rate diminished or even negatively affected tree growth rate through iWUE paths in the later period (Fig. 4b). Nutrient-induced structural overshoot[42] may be the primary factor that enhanced forest vulnerability to episodic water deficit accompanied by shaper growth decline in more fertile sites (Fig. 2c). However, although previous assessment showed no detrimental impacts on biological activities as we applied class-A biosolids with minimum levels of heavy metals[79], the accumulation of metals in soil may reduce stomata conductance and disturb plant water status from root to canopy through permeating calcium channels[80], potentially intensifying hydraulic failure. Such environmental issues may be pronounced in coastal regions of developing areas with increasing contaminated sedimentary inputs, implying that regional inequality of local stressors tends to complicate the global change scenario.

The iWUE-growth relationship, predictors, and consequences for tree mortality

Higher leaf N content can allow trees to have a higher investment in RuBisCO and other proteins involved in photosynthesis[51] for achieving a given carbon assimilation rate (A) with lower stomatal conductance under dry environmental conditions[81]. We observed unchanged leaf N for nutrient-enriched sites (Fig. 3e and Supplementary Fig. 12), suggesting an unchanged carbon assimilation rate (A), and thus, increased iWUE in these sites could be mainly ascribed to a tighter stomatal regulation. Instead, trees not exposed to nutrient enrichment exhibiting concave-positive shifts in leaf N and iWUE (Fig. 3e) may indicate a more flexible stomatal regulation due to less extensive water shortage. The initial decline of leaf N may be ascribed to a dilution of N in leaf tissues by increased photosynthetic compounds during a fast-growing period and a shortage of root N uptake[82], while the later increase of leaf N may be ascribed to a shift from N to water limitation with rising water deficit (Fig. 4). For fertile sites, nutrient enrichment likely diminished this dilution effect, however, severe reductions in stomatal conductance (g_s) could substantially enhance iWUE in the later period, with groundwater salinity emerging as the predominant factor (Fig. 4 and Supplementary Fig. 7). Declining net carbon gains despite rising iWUE ultimately dampens the positive coupling of iWUE and tree annual growth rates (BAI) (Fig. 3f)[74], as also observed in other coastal forests following seawater exposure[30,31]. Ultimately, a decrease in tree carbon–water coordination may increase forest vulnerability to air dryness and accelerate the risk of tree mortality once hydraulic failure couples with progressive carbon starvation[7,15], as shown by the significantly enhanced mortality in the later period (Supplementary Fig. 9).

Because of the disproportionately high influence of local factors than climates with regard to the proposed physiological framework (Fig. 4c), declines in tree growth rate could potentially increase their susceptibility to mortality risk. Particularly, the negative impact of mismatches between water demand and supply on tree growth can be exacerbated by tree competition. Trees under high competition levels often have increased negative water potential and lower soil-to-leaf hydraulic conductance and stomatal conductance[83]. In line with the aforementioned, we observed stronger negative iWUE-BAI feedback under high stand density (Fig. 2c). Elevated nutrient availability can initially result in a series of shifts in plant hydraulic traits, such as increased leaf area and transpiration rates but reduced carbon (C) investment in roots, resulting in an overall decline in root biomass and mycorrhizal association[43], as observed in our previous studies in this experimental trial[84,85]. These changes can induce greater water requirements but progressively hamper their water uptake capacity[37–39], thus exacerbating the coupled atmospheric and groundwater-related aridity in the later period and resulting in stronger negative iWUE-BAI feedback (Fig. 2c; Fig. 4). Consistent with this, although nutrient inputs promote annual tree growth during the whole experiment period (Figs. 1 and 4), fertile sites and high stand density exhibited high rates of tree mortality (Fig. 2d).

Taken together, to achieve optimal carbon–water balance and ensure hydraulic safety, photosynthetic regulation and shifts to deeper water resources may serve as acclimation strategies to the recent acceleration of atmospheric drought scenarios in coastal areas. Nevertheless, by leveraging the negative impacts of ongoing atmospheric dryness, prolonged sea level rise accompanied by groundwater salinization would substantially accelerate coastal forest degradation, particularly in formerly crowded and fertile areas. These findings uncover the overlooked leverage effect of local stressors and belowground drivers[10] that would outcompete climate factors to accelerate future coastal vegetation transitions[4] and compromise global carbon sink capacity[8,9].

Data availability

All data that supports the findings of this study are publicly available at the Figshare data repository (https://doi.org/10.6084/m9.figshare.30415954)[86].

Code availability

No custom code or algorithm was developed in this study. All plotting codes are available from corresponding author upon request.

Received: 17 August 2024; Accepted: 13 November 2025;
Published online: 26 November 2025

References

1. Nicholls, R. J. & Cazenave, A. Sea-level rise and its impact on coastal zones. *Science* **328**, 1517–1520 (2010).
2. Small, C. & Nicholls, R. J. A global analysis of human settlement in coastal zones. *J. Coast. Res.* **19**, 584–599 (2003).
3. Ward, N. D. et al. Representing the function and sensitivity of coastal interfaces in Earth system models. *Nat. Commun.* **11**, 1–14 (2020).
4. Chen, Y. & Kirwan, M. L. Climate-driven decoupling of wetland and upland biomass trends on the mid-Atlantic coast. *Nat. Geosci.* **15**, 913–918 (2022).
5. Ury, E. A., Yang, X., Wright, J. P. & Bernhardt, E. S. Rapid deforestation of a coastal landscape driven by sea-level rise and extreme events. *Ecol. Appl.* **31**, e02339 (2021).
6. Kirwan, M. L. & Gedan, K. B. Sea-level driven land conversion and the formation of ghost forests. *Nat. Clim. Change* **9**, 450–457 (2019).
7. McDowell, N. G. et al. Processes and mechanisms of coastal woody-plant mortality. *Glob. Change Biol.* **28**, 5881–5900 (2022).
8. Rosentreter, J. A. et al. Coastal vegetation and estuaries are collectively a greenhouse gas sink. *Nat. Clim. Change* **13**, 579–587 (2023).
9. Kirwan, M. L., Megonigal, J. P., Noyce, G. L. & Smith, A. J. Geomorphic and ecological constraints on the coastal carbon sink. *Nat. Rev. Earth Environ.* **4**, 393–406 (2023).
10. Regier, P. et al. Short-term experimental flooding impacts soil biogeochemistry but not aboveground vegetation in a coastal forest. *Proc. Natl. Acad. Sci. USA* **122**, e2511756122 (2025).
11. Denissen, J. M. et al. Widespread shift from ecosystem energy to water limitation with climate change. *Nat. Clim. Change* **12**, 677–684 (2022).
12. Yuan, W. et al. Increased atmospheric vapor pressure deficit reduces global vegetation growth. *Sci. Adv.* **5**, eaax1396 (2019).

13. Humphrey, V. et al. Soil moisture–atmosphere feedback dominates land carbon uptake variability. *Nature* **592**, 65–69 (2021).
14. Green, J. K. et al. Large influence of soil moisture on long-term terrestrial carbon uptake. *Nature* **565**, 476–479 (2019).
15. Ding, J. et al. Modeling the mechanisms of conifer mortality under seawater exposure. *New Phytol.* **239**, 1679–1691 (2023).
16. Giguère-Croteau, C. et al. North America's oldest boreal trees are more efficient water users due to increased [CO2], but do not grow faster. *Proc. Natl. Acad. Sci. USA* **116**, 2749–2754 (2019).
17. Van Der Sleen, P. et al. No growth stimulation of tropical trees by 150 years of CO2 fertilization but water-use efficiency increased. *Nat. Geosci.* **8**, 24–28 (2015).
18. Peñuelas, J., Canadell, J. G. & Ogaya, R. Increased water-use efficiency during the 20th century did not translate into enhanced tree growth. *Glob. Ecol. Biogeogr.* **20**, 597–608 (2011).
19. Martínez-Sancho, E. et al. Increased water-use efficiency translates into contrasting growth patterns of Scots pine and sessile oak at their southern distribution limits. *Glob. Change Biol.* **24**, 1012–1028 (2018).
20. Chen, Z., Wang, W., Forzieri, G. & Cescatti, A. Transition from positive to negative indirect CO2 effects on the vegetation carbon uptake. *Nat. Commun.* **15**, 1500 (2024).
21. Costa, F. R., Schietti, J., Stark, S. C. & Smith, M. N. The other side of tropical forest drought: do shallow water table regions of Amazonia act as large-scale hydrological refugia from drought?. *N. Phytol.* **237**, 714–733 (2023).
22. Sousa, T. R. et al. Water table depth modulates productivity and biomass across Amazonian forests. *Glob. Ecol. Biogeogr.* **31**, 1571–1588 (2022).
23. Wang, J., Taylor, A. R. & D'Orangeville, L. Warming-induced tree growth may help offset increasing disturbance across the Canadian boreal forest. *Proc. Natl. Acad. Sci. USA* **120**, e2212780120 (2023).
24. Williams, J. et al. Local groundwater decline exacerbates response of dryland riparian woodlands to climatic drought. *Glob. Change Biol.* **28**, 6771–6788 (2022).
25. Santos, I. R. et al. Submarine groundwater discharge impacts on coastal nutrient biogeochemistry. *Nat. Rev. Earth Environ.* **2**, 307–323 (2021).
26. Cuthbert, M. et al. Global patterns and dynamics of climate–groundwater interactions. *Nat. Clim. Change* **9**, 137–141 (2019).
27. Li, W. et al. The influence of increasing atmospheric CO2, temperature, and vapor pressure deficit on seawater-induced tree mortality. *N. Phytol.* **235**, 1767–1779 (2022).
28. Rajanayaka, C., Weir, J., Kerr, T. & Thomas, J. Sustainable water resource management using surface-groundwater modelling: Motueka-Riwaka Plains, New Zealand. *Watershed Ecol. Environ.* **3**, 38–56 (2021).
29. Callander, P., Lough, H. & Steffens, C. New Zealand guidelines for the monitoring and management of sea water intrusion risks on groundwater. *Envirolink Proj.* 82–87 (2011).
30. Wang, W. et al. Constrained tree growth and gas exchange of seawater-exposed forests in the Pacific Northwest, USA. *J. Ecol.* **107**, 2541–2552 (2019).
31. Kubota, T., Kagawa, A. & Kodama, N. Effects of salt water immersion caused by a tsunami on δ13C and δ18O values of Pinus thunbergii tree-ring cellulose. *Ecol. Res.* **32**, 271–277 (2017).
32. Werner, A. D. et al. Seawater intrusion processes, investigation and management: recent advances and future challenges. *Adv. Water Resour.* **51**, 3–26 (2013).
33. Fan, Y., Li, H. & Miguez-Macho, G. Global patterns of groundwater table depth. *Science* **339**, 940–943 (2013).
34. Qiu, J. et al. Nonlinear groundwater influence on biophysical indicators of ecosystem services. *Nat. Sustain.* **2**, 475–483 (2019).
35. Grossiord, C. et al. Warming combined with more extreme precipitation regimes modifies the water sources used by trees. *N. Phytol.* **213**, 584–596 (2017).
36. Bauman, D. et al. Tropical tree mortality has increased with rising atmospheric water stress. *Nature* **608**, 528–533 (2022).
37. Gessler, A., Schaub, M. & McDowell, N. G. The role of nutrients in drought-induced tree mortality and recovery. *N. Phytol.* **214**, 513–520 (2017).
38. Brooks, J. R. & Coulombe, R. Physiological responses to fertilization recorded in tree rings: isotopic lessons from a long-term fertilization trial. *Ecol. Appl.* **19**, 1044–1060 (2009).
39. Liang, X. et al. Global response patterns of plant photosynthesis to nitrogen addition: a meta-analysis. *Glob. Change Biol.* **26**, 3585–3600 (2020).
40. Zhang, Y. et al. Soil nitrogen drives inverse acclimation of xylem growth cessation to rising temperature in Northern Hemisphere conifers. *Proc. Natl. Acad. Sci. USA* **122**, e2421834122 (2025).
41. Ellis, J., Hatton, C. & Lohrer, A. Muddy waters: elevating sediment input to coastal and estuarine habitats. *Front. Ecol. Environ.* **2**, 299–306 (2004).
42. Callahan, R. P. et al. Forest vulnerability to drought controlled by bedrock composition. *Nat. Geosci.* **15**, 714–719 (2022).
43. Eastman, B. A. et al. Altered plant carbon partitioning enhanced forest ecosystem carbon storage after 25 years of nitrogen additions. *N. Phytol.* **230**, 1435–1448 (2021).
44. Jump, A. S. et al. Structural overshoot of tree growth with climate variability and the global spectrum of drought-induced forest dieback. *Glob. change Biol.* **23**, 3742–3757 (2017).
45. Furniss, T. J., Das, A. J., van Mantgem, P. J., Stephenson, N. L. & Lutz, J. A. Crowding, climate, and the case for social distancing among trees. *Ecol. Appl.* **32**, e2507 (2022).
46. Zhang, J., Huang, S. & He, F. Half-century evidence from western Canada shows forest dynamics are primarily driven by competition followed by climate. *Proc. Natl. Acad. Sci. USA* **112**, 4009–4014 (2015).
47. Kunstler, G. et al. Effects of competition on tree radial-growth vary in importance but not in intensity along climatic gradients. *J. Ecol.* **99**, 300–312 (2011).
48. Fernández-de-Uña, L., McDowell, N. G., Cañellas, I. & Gea-Izquierdo, G. Disentangling the effect of competition, CO 2 and climate on intrinsic water-use efficiency and tree growth. *J. Ecol.* **104**, 678–690 (2016).
49. Gonzalez de Andres, E. et al. Tree-to-tree competition in mixed European beech–Scots pine forests has different impacts on growth and water-use efficiency depending on site conditions. *J. Ecol.* **106**, 59–75 (2018).
50. Luo, Y., McIntire, E. J., Boisvenue, C., Nikiema, P. P. & Chen, H. Y. Climatic change only stimulated growth for trees under weak competition in central boreal forests. *J. Ecol.* **108**, 36–46 (2020).
51. Smith, N. G. et al. Global photosynthetic capacity is optimized to the environment. *Ecol. Lett.* **22**, 506–517 (2019).
52. McCarroll, D. & Loader, N. J. Stable isotopes in tree rings. *Quat. Sci. Rev.* **23**, 771–801 (2004).
53. Farquhar, G. D., O'Leary, M. H. & Berry, J. A. On the relationship between carbon isotope discrimination and the intercellular carbon dioxide concentration in leaves. *Funct. Plant Biol.* **9**, 121–137 (1982).
54. Farquhar, G., Hubick, K., Condon, A. & Richards, R. in *Stable Isotopes in Ecological Research* 21–40 (Springer, 1989).
55. Craine, J. M. et al. Isotopic evidence for oligotrophication of terrestrial ecosystems. *Nat. Ecol. Evol.* **2**, 1735–1744 (2018).
56. Walker, A. P. et al. The relationship of leaf photosynthetic traits–Vcmax and Jmax–to leaf nitrogen, leaf phosphorus, and specific leaf area: a meta-analysis and modeling study. *Ecol. evol.* **4**, 3218–3235 (2014).
57. El-Madany, T. S. et al. How nitrogen and phosphorus availability change water use efficiency in a Mediterranean savanna ecosystem. *J. Geophys. Res. Biogeosci.* **126**, e2020JG006005 (2021).

58. McDowell, N. G. Mechanisms linking drought, hydraulics, carbon metabolism, and vegetation mortality. *Plant Physiol.* **155**, 1051–1059 (2011).
59. Hubau, W. et al. Asynchronous carbon sink saturation in African and Amazonian tropical forests. *Nature* **579**, 80–87 (2020).
60. Brienen, R. J. et al. Forest carbon sink neutralized by pervasive growth-lifespan trade-offs. *Nat. Commun.* **11**, 4241 (2020).
61. Oren, R. et al. Soil fertility limits carbon sequestration by forest ecosystems in a CO2-enriched atmosphere. *Nature* **411**, 469–472 (2001).
62. Zhang, Y. et al. High preseason temperature variability drives convergence of xylem phenology in the Northern Hemisphere conifers. *Curr. Biol.* **34**, 1161–1167.e1163 (2024).
63. Guerrieri, R. et al. The legacy of enhanced N and S deposition as revealed by the combined analysis of δ13C, δ18O and δ15N in tree rings. *Glob. Change Biol.* **17**, 1946–1962 (2011).
64. Norby, R. J. & Zak, D. R. Ecological lessons from free-air CO2 enrichment (FACE) experiments. *Ann. Rev. Ecol. Evol. Syst.* **42**, 181–203 (2011).
65. Terrer, C. et al. Nitrogen and phosphorus constrain the CO2 fertilization of global plant biomass. *Nat. Clim. Change* **9**, 684–689 (2019).
66. Jiang, M. et al. Low phosphorus supply constrains plant responses to elevated CO2: a meta-analysis. *Glob. Change Biol.* **26**, 5856–5873 (2020).
67. Perri, S. et al. River basin salinization as a form of aridity. *Proc. Natl. Acad. Sci. USA* **117**, 17635–17642 (2020).
68. Gessler, A. et al. Drought induced tree mortality–a tree-ring isotope based conceptual model to assess mechanisms and predispositions. *N. Phytol.* **219**, 485–490 (2018).
69. Deans, R. M., Brodribb, T. J., Busch, F. A. & Farquhar, G. D. Optimization can provide the fundamental link between leaf photosynthesis, gas exchange and water relations. *Nat. Plants* **6**, 1116–1125 (2020).
70. Smith, N. G. & Keenan, T. F. Mechanisms underlying leaf photosynthetic acclimation to warming and elevated CO2 as inferred from least-cost optimality theory. *Glob. Change Biol.* **26**, 5202–5216 (2020).
71. Farquhar, G. D., Cernusak, L. A. & Barnes, B. Heavy water fractionation during transpiration. *Plant Physiol.* **143**, 11–18 (2007).
72. Keenan, T. F. et al. Increase in forest water-use efficiency as atmospheric carbon dioxide concentrations rise. *Nature* **499**, 324–327 (2013).
73. Lavergne, A. et al. Historical changes in the stomatal limitation of photosynthesis: empirical support for an optimality principle. *N. Phytol.* **225**, 2484–2497 (2020).
74. Driscoll, A. W., Bitter, N. Q., Sandquist, D. R. & Ehleringer, J. R. Multidecadal records of intrinsic water-use efficiency in the desert shrub Encelia farinosa reveal strong responses to climate change. *Proc. Natl. Acad. Sci. USA* **117**, 18161–18168 (2020).
75. Ellsworth, P. V. & Sternberg, L. S. Biochemical effects of salinity on oxygen isotope fractionation during cellulose synthesis. *N. Phytol.* **202**, 784–789 (2014).
76. González de Andrés, E. et al. The role of nutritional impairment in carbon-water balance of silver fir drought-induced dieback. *Glob. Change Biol.* **28**, 4439–4458 (2022).
77. Herrero, A., Castro, J., Zamora, R., Delgado-Huertas, A. & Querejeta, J. I. Growth and stable isotope signals associated with drought-related mortality in saplings of two coexisting pine species. *Oecologia* **173**, 1613–1624 (2013).
78. Sarris, D., Siegwolf, R. & Körner, C. Inter-and intra-annual stable carbon and oxygen isotope signals in response to drought in Mediterranean pines. *Agric. For. Meteorol.* **168**, 59–68 (2013).
79. Xue, J. et al. Ecological impacts of long-term application of biosolids to a radiata pine plantation. *Sci. Total Environ.* **530**, 233–240 (2015).
80. Perfus-Barbeoch, L., Leonhardt, N., Vavasseur, A. & Forestier, C. Heavy metal toxicity: cadmium permeates through calcium channels and disturbs the plant water status. *Plant J.* **32**, 539–548 (2002).
81. Querejeta, J. I. et al. Higher leaf nitrogen content is linked to tighter stomatal regulation of transpiration and more efficient water use across dryland trees. *N. Phytol.* **235**, 1351–1364 (2022).
82. Taub, D. R. & Wang, X. Why are nitrogen concentrations in plant tissues lower under elevated CO2? A critical examination of the hypotheses. *J. Integr. Plant Biol.* **50**, 1365–1374 (2008).
83. MORENO-GUTIÉRREZ, C. et al. Stand structure modulates the long-term vulnerability of Pinus halepensis to climatic drought in a semiarid Mediterranean ecosystem. *Plant Cell Environ.* **35**, 1026–1039 (2012).
84. Wang, M., Xue, J., Horswell, J., Kimberley, M. O. & Huang, Z. Long-term biosolids application alters the composition of soil microbial groups and nutrient status in a pine plantation. *Biol. Fertil. Soils* **53**, 799–809 (2017).
85. Wang, M., Zhang, Y., Huang, Z., Xue, J. & Gutierrez-Gines, M. J. Limited potential of biosolids application for long-term soil carbon stabilization in coastal dune forests. *Geoderma* **403**, 115384 (2021).
86. Wang, M. A long-term experiment showed how coastal groundwater salinization impaired tree carbon–water balance. Figshare https://doi.org/10.6084/m9.figshare.30415954 (2025).

Acknowledgements

This study was funded by GDAS' Project of Science and Technology Development (2024GDASZH-2024010101), the National Natural Science Foundation of China (Grant no. 32271653), Guangdong Natural Science Foundation (Grant no. 2023A1515010638) and Guangdong S&T Program (2025A04J4461). It was initiated in a working group (led by M.W. and J.X.) that was supported by Scion, New Zealand. N.G.M. was supported by the Department of Energy's Coastal Observations, Mechanisms, and Predictions Across Systems and Scales (COMPASS). The authors thank PF Olsen Limited, Tasman District Council, the Nelson Regional Sewerage Business Unit, and the New Zealand Ministry of Business, Innovation and Employment for funding (Contract no. C03X0902) or in-kind support; Doug Graham, Alan Leckie and David Henley for field sampling and growth measurement; Peter Wilks at PF Olsen for trial maintenance; and all those who have contributed to the project over the years.

Author contributions

M.W. and J.X. designed the study. Y.Z. and M.W. performed the analysis and drafted the paper. J.P., N.M., J.X., Z.H., and X.G. contributed to the interpretation of the results and the writing of the paper.

Competing interests

The authors declare no competing interests.

Additional information

Supplementary information The online version contains supplementary material available at https://doi.org/10.1038/s43247-025-03032-3.

Correspondence and requests for materials should be addressed to Minhuang Wang.

Peer review information *Communications Earth and Environment* thanks Eladio Cornejo-Oviedo and the other, anonymous, reviewer(s) for their contribution to the peer review of this work. Primary Handling Editors: Mengjie Wang. [A peer review file is available].